

reported for a variety of gastropod shells, whose SM's were resolved as several proteins, all with molecular weights lower than that reported here (2).

Calcium-binding studies were performed on matrix solutions that had been redialyzed, first against 1 mM EDTA (pH 7.5) and then against water. Redialysis removed residual calcium from matrix preparations. The binding capacity of the protein was determined by measuring the decrease in free calcium in 10 ml of 10^{-3} to 10^{-4} M CaCl_2 (pH 6.0) when matrix protein (3 to 150 μg) was added (11). For all preparations, the quantity of calcium removed from solution was directly proportional to the quantity of protein added and was independent of calcium concentration in the range of 10^{-3} to 10^{-4} M, indicating that the protein was saturated with calcium during the experiments. The mean binding capacity for four preparations (two EDTA-extracted and two HCl-extracted) was 23.2 ± 2.92 μmole of calcium per milligram of protein (mean \pm standard error). This is considerably higher than the 0.65 $\mu\text{mole}/\text{mg}$ obtained for SM from clams (12). The difference may result in part from estimation of SM on the basis of protein content, since protein constitutes an unknown portion of the matrix molecule, or it may be related to differences in techniques for estimating amounts of matrix and protein. That the SM of oyster acts as an effective calcium-binding protein, though, is in general agreement with the findings for clam SM. The inhibiting effect on crystal nucleation and growth is not simply due to removal of calcium, however, because at an SM concentration of 7.94 $\mu\text{g}/\text{ml}$ (Fig. 1) less than 2 percent of calcium in the medium is bound.

The effect of SM on CaCO_3 precipitation is apparently specific for the matrix protein. When phosphovitin (Sigma), a phosphoprotein that inhibits calcium phosphate crystal growth (13), was tested in this system (Fig. 1C) only slight inhibition of the rate and negligible inhibition of the initiation of precipitation were observed, and then only with quantities of phosphovitin greater than the quantities of matrix normally employed in these experiments. Similarly, up to 1.5 μmole (0.3 ml of 5.0 mM) EDTA had no effect on the rate of precipitation or the time required for initiation of precipitation (data not shown).

The results reported here directly demonstrate regulation of crystal nucleation and growth by a protein in a CaCO_3 system. Such regulation by calcium-binding proteins has been demonstrated

for calcium phosphate systems and has been proposed for components of insoluble (14-16) and soluble (4) matrix of molluscan shell. The results do not favor a role for calcium-binding SM in initiating crystal growth, nor do they exclude it. However, one might have expected an effect on precipitation if initiation were the primary function of the protein.

Exactly how the matrix protein binds to a forming crystal is not known. However, it is tempting to speculate that the multiple binding sites for calcium present on these proteins might interact with the nucleation site or surface of the forming crystal in such a way as to prevent further accretion of mineral, presumably by raising the free energy for activation of this process. For this protein-crystal association to occur, the protein must have a much higher affinity for the crystal than for free calcium, as the binding sites on the protein would normally be saturated with calcium from solution.

In summary, SM from molluscan shells has the potential to regulate CaCO_3 deposition. Control of crystal growth thus seems to depend on control of SM secretion or activation, processes about which virtually nothing is known.

A. P. WHEELER
JAMES W. GEORGE
C. A. EVANS

Department of Zoology,
Clemson University,
Clemson, South Carolina 29631

Improved Detail in Biological Soft X-ray Microscopy: Study of Blood Platelets

Abstract. Improved image quality in soft x-ray contact microscopy can be obtained by examining the resist with transmission rather than scanning electron microscopy. Application of the new technique to air-dried preparations of human blood platelets reveals structures not visible in the same cells with transmission electron microscopy or when the resist is examined by scanning electron microscopy. As seen by the new technique, platelet pseudopods contain a central structure connected to a network in the platelet and dense bodies exhibit a lamellar structure.

Contact x-ray microscopy is an excellent imaging technique for use in biological studies (1). It has several advantages over other imaging techniques currently in use. Resolutions in the range of 5 nm can be achieved with relatively thick and hydrated specimens, and information about the subcellular distribution of light elements can be obtained from their absorbance or fluorescence properties. In addition, staining is not required to obtain relatively good contrast in biological structures, and imaging is possible at radiation doses somewhat lower than those needed for imaging with electrons.

References and Notes

1. M. A. Crenshaw, *Biomaterialization* 6, 6 (1972).
2. G. Krampitz, J. Engels, C. Cazaux, in *The Mechanisms of Mineralization in the Invertebrates and Plants*, N. Watabe and K. M. Wilbur, Eds. (Univ. of South Carolina Press, Columbia, 1976), p. 155.
3. S. Weiner, *Calcif. Tissue Int.* 29, 163 (1979).
4. M. A. Crenshaw and H. Ristedt, in *The Mechanisms of Mineralization in the Invertebrates and Plants*, N. Watabe and K. M. Wilbur, Eds. (Univ. of South Carolina Press, Columbia, 1976), p. 355.
5. G. L. Miller, *Anal. Chem.* 31, 964 (1959).
6. The overall reaction for precipitation is $\text{Ca}^{2+} + \text{HCO}_3^- \rightarrow \text{CaCO}_3 + \text{H}^+$. The decrease in pH was followed with a Fisher miniature glass electrode (13-639-77), a Beckman miniature reference electrode (41239), a Fisher pH meter (Accumet, model 420), and a potentiometric recorder. The reaction medium was stirred continuously.
7. G. Fairbanks, T. L. Steck, D. F. H. Wallack, *Biochemistry* 10, 2606 (1971).
8. Preliminary results indicate that at pH greater than 8.7 (and thus higher carbonate concentrations) greater protein concentrations are required to significantly inhibit initiation of crystal growth.
9. M. Bradford, *Anal. Biochem.* 72, 248 (1976).
10. P. G. Righetti and F. Chillemi, *J. Chromatogr.* 157, 253 (1978).
11. The decrease in free calcium was determined with a calcium electrode (Orion, series 93) and a calomel reference electrode. The test solutions usually contained 100 μg of bovine serum albumin (Sigma) to displace matrix protein from the vessel wall. This was necessary because of the small quantities of matrix protein used.
12. This was calculated from data in (1). Binding capacity was expressed as micromoles of Ca^{2+} bound per micromole of matrix sulfate, with sulfate and protein estimated as 9.9 and 79.5 percent of the matrix by weight, respectively.
13. J. D. Termine, E. D. Eanes, K. M. Conn, *Calcif. Tiss. Int.* 31, 247 (1980).
14. N. Watabe, *J. Ultrastruct. Res.* 1, 351 (1965).
15. K. M. Towe and G. H. Hamilton, *Calcif. Tiss. Res.* 1, 306 (1968).
16. G. Bevelander and H. Nakahara, *ibid.* 3, 84 (1969).
17. We thank D. Dillaman and S. Sikes for commenting on the manuscript. Supported by NSF grant PCM79-16587.

31 March 1981

the transmission electron microscope (TEM). The theoretical resolution of the resist technique and accurate quantitation of the absorption properties of the specimen can now be attained with relative ease.

To examine developed x-ray resists with transmitted electrons, an ultrathin substrate must be formed which is capable of supporting the very thin layer of resist material. A 100-nm film of Si_3N_4 with the necessary substrate properties (flat, strong, and relatively transparent to soft x-rays and to electrons in the 60- to 100-keV range) is formed by chemical vapor deposition on the polished surface of a silicon wafer. Holes are back-etched in the wafer, leaving an amorphous Si_3N_4 film approximately 100 nm thick supported by a silicon frame (2). Then 400 to 800 nm of x-ray resist (polymethyl methacrylate or copolymer) is spun onto the flat Si_3N_4 surface in the conventional manner. Specimens on electron microscope grids are placed in contact with the resist and exposed in a soft x-ray source (Fig. 1) (1). Exposed resists are developed and may be coated with a thin (10-nm) layer of gold and palladium or examined directly in the electron microscope without further treatment. To minimize electron beam heating of uncoated resists, they must be developed to a point where the maximal thickness is less than 400 nm. In practice, this can be done by developing the resists for brief periods and monitoring the thickness of an essentially unexposed portion (the image of the grid bars) with an interference microscope.

Although examination of hydrated cells is possible in the x-ray source used,

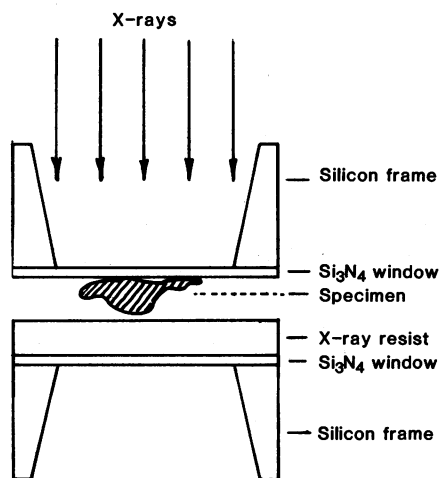


Fig. 1. Schematic diagram showing specimen mounted on a thin window of Si_3N_4 . Transmitted x-rays expose a thin polymeric resist spun onto a similar Si_3N_4 window, which, after development of the resist, is retained as an electron-transmitting substrate.

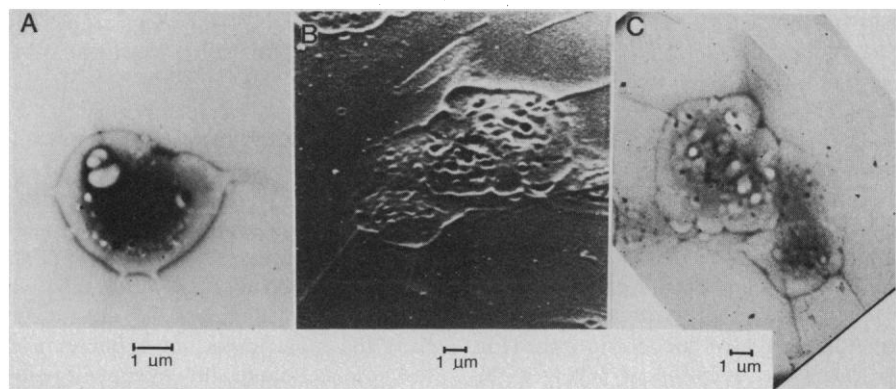


Fig. 2. (A) Transmission electron micrograph of an air-dried whole mount of a human blood platelet with several pseudopods extending out from the cell body. Dense bodies are dark, circular structures, and the cell margin is outlined by a dense rim of dried protein (4). (B) Scanning electron micrograph of a metallized x-ray replica of air-dried blood platelets showing two platelets with pseudopods. The dense bodies and vacuoles are seen as protrusions and depressions, respectively. (C) Transmission electron micrograph of the same replica. All pseudopods exhibit backbone-like structures that intersect a periplaetlet structure of similar density; in some cases the pseudopod core extends into the substance of the platelet. To permit SEM examination of this specimen, the resist was coated with 10 nm of gold and palladium. Similar detail was seen in unmetallized resists.

a relatively long exposure time in a hypoxic environment is required (10 to 12 hours) (3). We chose air-dried whole mounts of human blood platelets for testing because they have been extensively characterized by electron microscopy and because they appear to possess all the morphological features described in fixed and sectioned material (4). Platelets were dried on grids coated with 20 nm of amorphous carbon and irradiated with carbon K_α x-rays (4.4-nm wavelength) as described above (1). X-ray resists were then examined by scanning and transmission electron microscopy and compared with transmission images of the same cells.

There are striking differences in the amount and type of ultrastructural detail discernible in each preparation (Fig. 2). The grid coating and the Si_3N_4 window attenuated the incident x-rays equally over the entire specimen and thus contributed virtually nothing to the images seen in the developed resists. Platelet dense bodies viewed in the TEM appear as electron-opaque structures with sharply demarcated edges and a relatively homogeneous internal core (Fig. 2A) (4). Pseudopods projecting from the cells show the suggestion of a core structure only toward their tips, with a relatively homogeneous base merging into the platelet cytoplasm. Other structures inside the cells are more poorly defined, and no evidence of an internal network is apparent. Platelet images in resist studied by the SEM (Fig. 2B) show smooth-contoured bulbous projections that correspond in location to dense bodies—an appearance probably due to relatively high absorption of the incident photons

by calcium, phosphorus, and oxygen in the dense body core (4). Pseudopods and a periplaetlet rim are also visible as smooth, raised topological features, although their relations to the actual cell boundaries are not apparent. When the same resist is studied with transmitted electrons (Fig. 2C), the dense bodies appear as lamellated rather than homogeneous structures and contain small clumps of material scattered throughout the core. Since the cell and pseudopod edges are more clearly defined in this image, it is apparent that each pseudopod contains a photon-absorbent core. The pseudopod core appears to intersect a rim of similar material lying just inside the cell periphery, and in many cases the

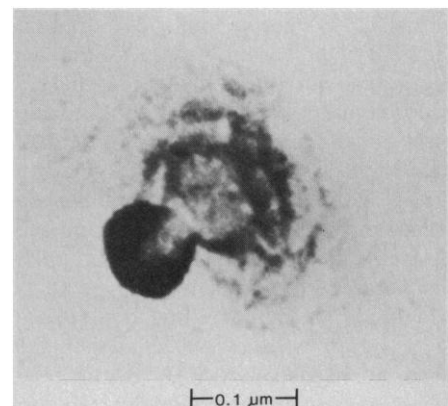


Fig. 3. High magnification transmission electron micrograph of a dense body as seen in a developed x-ray resist. The dense body appears to have a lamellar structure and contains particulate inhomogeneities. The background is due to a noncontinuous metal coating. Dark object to the lower left of the dense body is probably a foreign particle in the resist.

core extends into the cytoplasm. In addition, the cytoplasm contains a network of photon-absorbent material that surrounds vacuoles, connects with dense bodies, and, in some cases, appears to be continuous with the pseudopod core. Platelets fixed in glutaraldehyde before the preparation of whole mounts show similar morphological detail in both dense bodies and pseudopods.

The fact that resist dense bodies appear to consist of concentric rings (Fig. 3) raises the question of whether this ultrastructure is unique to the resist, exists in the living state, or is introduced in the whole mount during the air-drying procedure. It probably is not an artifact of the exposure and development processes, since other regions of high photon absorption (such as the pericytoplasmic rim and the pseudopod core) are reproduced in the resist as smooth structures. In addition, TEM examination of the same platelets before and after x-irradiation for periods of 8 to 100 hours showed no obvious structural differences. If the lamellar arrangement exists in vivo, it may occur by sequential precipitation of secreted material as the dense body is formed in the megakaryocyte. An explanation of why it is not visible by TEM in the actual whole mount is lacking, however.

Two other features visible in the resist but not in the whole mount may owe their prominence in the resist to differences in the cross section for electron scattering versus photon absorption. In passing from carbon to sulfur (atomic numbers 6 to 16), the total electron scattering cross section for 100-keV electrons rises by a factor of approximately 3, while the absorption cross section for 4.4-nm photons rises by a factor of 50. Thus a PO₄ group looks like approximately eight carbon atoms to 100-keV electrons but looks like more than 50 carbon atoms to 4.4-nm photons. Platelets contain large quantities of actin, a molecule associated in its polymerized form with one adenosine diphosphate molecule. Pseudopods in fixed and sectioned platelets appear to contain a filamentous core, which is believed to be composed of actin, although a specific connection with cytoplasmic elements has not been convincingly documented (5). If the cytoplasmic network, the periplasmic rim, and the pseudopod core represent adenosine diphosphate-associated actin relatively rich in phosphorus and oxygen, they would be essentially indistinguishable to 100-keV electrons when embedded in a proteinaceous matrix, but significantly more absorbent than their surround to 4.4-nm photons.

Transmission electron microscope images of x-ray resists made from other cells or tissues may provide new insights into subcellular organization, since they can highlight features not readily visible with conventional electron microscopy (6). Resists may now be examined with a resolution approaching 5 nm and, with proper equipment, can provide qualitative information about elements that may be present in small cellular areas. Perhaps the most important application of the new technique, however, will result from accurate quantitation of photon absorbance in areas of resists made with x-rays just below and above the absorption edges of elements of interest (7). By superimposition or subtraction of images obtained in this fashion, contact x-ray microscopy may provide a valuable tool for the quantitative imaging of the distribution of elements in biological specimens.

RALPH FEDER

IBM Watson Research Center,
Yorktown Heights, New York 10598

JONATHAN L. COSTA

Clinical Neuropharmacology Branch,
National Institute of Mental Health,
Bethesda, Maryland 20205

PRAVEEN CHAUDHARI, DAVID SAYRE
IBM Watson Research Center

References and Notes

1. P. Goby, *C. R. Acad. Sci.* **156**, 686 (1913); E. Spiller, R. Feder, J. Topalian, D. Eastman, W. Gudat, D. Sayre, *Science* **191**, 1172 (1976); R. Feder, E. Spiller, J. Topalian, A. N. Broers, W. Gudat, B. J. Panessa, Z. A. Zadunaisky, J. Sedat, *ibid.* **197**, 259 (1977); D. Sayre, J. Kirz, R. Feder, D. M. Kim, E. Spiller, *ibid.* **196**, 1339 (1977). For a review see J. Kirz and D. Sayre, in *Synchrotron Radiation Research*, H. Winick and S. Doniach, Eds. (Plenum, New York, 1980).
2. E. Bassous, R. Feder, E. Spiller, J. Topalian, *Solid State Technol.* **19**, 55 (1976); H. I. Smith and D. C. Flanders, *Jpn. J. Appl. Phys.* **16** (Suppl.), 61 (1977).
3. Resist replicas of hydrated biological specimens may be produced by using a flash x-ray source with an x-ray output sufficient to expose the resist in a few nanoseconds [R. McCorkle *et al.*, *Science* **205**, 401 (1979)].
4. J. G. White, *Ser. Haematol.* **3**, 17 (1970); J. L. Costa, T. S. Reese, D. L. Murphy, *Science* **183**, 537 (1974); R. J. Skaer, P. D. Peters, J. P. Emmines, *J. Cell. Sci.* **20**, 441 (1976); J. L. Costa, Y. Tanaka, K. D. Pettigrew, R. J. Cushing, *J. Histochem. Cytochem.* **25**, 1079 (1977); S. W. Hui and J. L. Costa, *J. Microsc. (Oxford)* **115**, 203 (1979); D. C. Joy and D. M. Maher, *Science* **206**, 162 (1979).
5. J. H. Hartwig and T. P. Stossel, *J. Biol. Chem.* **250**, 5695 (1975); J. G. White and J. M. Gerrard, *Am. J. Pathol.* **83**, 590 (1976); D. Zucker-Franklin, *J. Clin. Invest.* **48**, 167 (1969).
6. In preliminary experiments, replicas made by TEM from whole mounts of fixed *Acanthamoeba castellanii* show vacuoles and bundles of filaments. Cultured cells, lymphocytes, and bacteria have also been examined.
7. Quantitation can be achieved by simultaneous exposure of a biological specimen and a wedge composed of a step series of Mylar films of known thicknesses. The electron scattering power of areas in the developed resist corresponding to the wedge series of Mylar films can then be used to derive the photon absorbance of the specimen.

13 March 1981

Estradiol and Progesterone Profiles Indicate a Lack of Endocrine Recognition of Pregnancy in the Opossum

Abstract. Concentrations of estradiol and progesterone in blood collected during the 12.5-day gestation period of the Virginia opossum were not significantly different from those during equivalent days of the estrous cycle. Progesterone was correlated with an index of corpora luteal mass. Ratios of estradiol to progesterone were highest 3 to 4 days before estrus and on the day of parturition.

As representatives of evolutionary lines that have been separate for over 80 million years (1), members of the infraclasses Metatheria (marsupials) and Eutheria (all other viviparous mammals, for example, primates, rodents, or ungulates) exhibit fundamentally different strategies for gestation and lactation. Eutherians deliver large, well-developed neonates after a relatively long gestation period that interrupts the estrous cycle and effects major alterations in maternal physiology. The corpus luteum of pregnancy is usually maintained beyond its normal life-span in the estrous cycle (2), and progesterone concentrations remain high until near parturition. Likewise, profiles (concentrations plotted over time) of circulating estrogens in eutherian gestation are high and qualitatively different from those seen during

the estrous cycle. In contrast, marsupials give birth to extremely small, embryonic young after a relatively short gestation and lactate for an extended period, several times longer than the period of gestation. In all but a few macropods (kangaroos and wallabies), the gestation period of marsupials is shorter than the estrous cycle, and if nurslings are taken from the mother after birth, estrous cycles continue unaltered (3).

Sharman (3) suggested that the estrous cycle might be hormonally equivalent to gestation in marsupials, a hypothesis based on anatomical and histological comparisons of reproductive tracts, embryo transfer experiments (4), and the temporal coincidence of estrous and gestational cycles. Our test of the equivalence hypothesis predicted no differences between these two reproductive